

Mixed alkylthiophene-based heterocyclic polymers containing oxadiazole units *via* electrochemical polymerisation: spectroscopic, electrochemical and spectroelectrochemical properties

Alexander S. Fisyuk,^{†a} Renaud Demadrille,^a Claudia Querner,^a Malgorzata Zagorska,^b Joël Bleuse^c and Adam Pron^{**a}

^a *Laboratoire de Physique des Métaux Synthétiques, DRFMC (CEA-CNRS-Université J. Fourier Grenoble I UMR 5819 SPram), CEA Grenoble, 17 Rue des Martyrs, 38054 Grenoble cedex 9, France. E-mail: pron@cea.fr; Fax: +33 438 785113; Tel: +33 438 784389*

^b *Faculty of Chemistry, Warsaw University of Technology, Noakowskiego 3, 00 664 Warszawa, Poland*

^c *Laboratoire Nanophysique des Semiconducteurs, DRFMC, SP2M, CEA Grenoble, 17 Rue des Martyrs, 38054 Grenoble cedex 9, France*

Received (in Montpellier, France) 7th October 2004, Accepted 10th January 2005
First published as an Advance Article on the web 23rd March 2005

Symmetric alkylthiophene-based mixed heterocyclic trimer and pentamer, containing central oxadiazole units, have been prepared. Because of the electron-withdrawing properties of oxadiazole, the trimer cannot be electropolymerised and undergoes an oxidative-type destruction at high potentials. In contrast, the pentamer readily polymerises, giving a short chain polymer. Both trimer and pentamer exhibit strong photoluminescence with a maximum at 399 nm (13% quantum yield) and 467 nm (46% quantum yield), respectively. The polymer resulting from the electropolymerisation of the pentamer is also luminescent with the maximum of the excitation band at 528 nm (33% quantum yield). The polymer can be oxidatively doped as demonstrated by cyclic voltammetry, showing a clear anodic peak at 0.62 V *versus* Ag/Ag⁺ and its cathodic counterpart at 0.56 V, associated with the undoping process. The significantly higher potential of the oxidative doping of the prepared mixed heterocyclic polymer, as compared to the poly(alkylthiophene) homopolymer of similar molecular weight, is caused by the presence of the oxadiazole unit, which lowers the electron density in the π -electron system of the oligothiophene subunit and makes its oxidation more difficult. The spectroelectrochemical investigation of the polymer is consistent with its voltammetric behaviour, exhibiting doping-induced bleaching of the band originating from the π - π^* transition and simultaneous growth of the bipolaron bands. The observed clear and reversible spectroelectrochemical behaviour makes the developed polymer a promising candidate for applications in electrochromic devices or electrochemical sensors.

Introduction

Conjugated oligomers and polymers have been extensively studied since more than two decades for three main reasons. First, in their doped (charged) state, they behave as organic conductors showing, in some cases, a very high electronic conductivity of the metallic type.¹ Second, in their undoped (neutral) state conjugated oligomers or polymers are organic semiconductors and, for this reason, they can serve as the main constituents of active elements in organic electronic devices such as field effect transistors (FETs), light-emitting diodes and photovoltaic cells, to name a few.² Third, conjugated monomers and oligomers frequently electropolymerise, giving polymers that can be electrochemically switched between the doped and the undoped states. Since the switching involves extremely pronounced and reversible changes in their physical properties, such as the electrical conductivity and the spectroscopic and magnetic properties among others, conjugated polymers can serve as electrochemical sensors of various types.³

Heterocyclic monomers and oligomers, especially those from the pyrrole and thiophene family, are very well suited for

electrochemical polymerisation.⁴ In this case, the electrochemical and spectroelectrochemical properties of the resulting polymers can be conveniently tuned by the presence of electron-donating or electron-withdrawing side groups that influence the electron density in the main conjugated backbone.^{5a} Another approach involves the synthesis of mixed heterocyclic polymers in which electron-donating units coexist with electron-withdrawing ones in the polymer main chain.^{5b} Typical examples of such systems are copolymers containing thiophene and oxadiazole units.⁶

Electropolymerisation of monomers in which the oxadiazole ring is adjacent to the thiophene one may be difficult to achieve because of the acceptor character of oxadiazole, which makes the oxidative coupling of thiophene, *via* the α carbon, more difficult. Therefore, polymers containing thiophene and oxadiazole are prepared by a polycondensation reaction leading to a nonconjugated precursor polymer that is then transformed into its conjugated analogue with simultaneous formation of the oxadiazole rings. Moreover, the use of this method inevitably leads to the incorporation of a phenylene ring into the polymer backbone.^{6a-c}

To the best of our knowledge, no conjugated polymers consisting solely of thiophene and oxadiazole units have ever been reported to date. In this article, we demonstrate that it is

[†] Permanent address: Department of Chemistry, Omsk State University, Pr. Mira 55a, 644077 Omsk, Russia.

possible to obtain such polymers *via* simple electropolymerisation of specially designed monomers.

Experimental

Materials and characterisation methods

All reagents were purchased from Aldrich and used as received. The synthesised products were characterised by ^1H and ^{13}C NMR spectroscopy, FT-IR spectroscopy, mass spectroscopy and elemental analysis. NMR spectra were recorded on a Bruker AC200 spectrometer. Chloroform-*d*, containing tetramethyl silane as internal standard, was used as solvent. Elemental analyses were carried out by the analytical service of the CNRS in Vernaison (France). FT-IR spectra were recorded on a Perkin Elmer Paragon 500 spectrometer (wavenumber range: 4000–400 cm^{-1} , resolution 2 cm^{-1}) using the ATR technique. Melting points were measured on a Büchi 510 apparatus.

Photoluminescence measurements of the monomers and the polymer in solution were carried out on an AvaSpec-2048-2 spectrofluorometer using a blue 400 nm diode or a UV lamp (254 nm, 25 W) for excitation. The photoluminescence quantum yields were determined by comparison with rhodamine 6G ($Q_f = 95\%$ in ethanol) or quinine sulfate ($Q_f = 54\%$ in 0.5 M sulfuric acid) using a dedicated setup, the excitation light being provided by a 10 μW Argon laser. The photoluminescence of the solid polymer film was measured only qualitatively. The excitation was performed with a 500 W deuterium lamp *via* a Jobin-Yvon Gemini 180 double monochromator. The variable wavelength excitation power output was in the range from 1 to 100 μW depending on the selected wavelength.

The molecular weight of polymer **P5** was determined using size exclusion chromatography (SEC) on a 1100HP Chemstation equipped with $300 \times 7.5 \text{ mm}^2$ PL gel mixed-D $5 \mu\text{m}/10^4 \text{ \AA}$ column. Detection was performed by a diode array UV-vis detector and a refractive index detector. The column temperature and the flow rate were fixed to 313 K and 1 ml min^{-1} , respectively. The calibration curve was built using ten polystyrene (PS) narrow standards (S-M-10* kit from Polymer Labs). Twenty microlitres of *ca.* 2 mg ml^{-1} polymer in THF (HPLC grade) were injected and analysed using a UV-vis detector at 355 nm.

Syntheses

3-Methylthiophene-2-carbonyl chloride (1). 3-Methylthiophene-2-carboxylic acid (14.2 g, 0.1 mol) was mixed with 60 ml of SOCl_2 in a reaction flask. The reaction mixture was boiled for approximately 2 h until the evolution of HCl was no longer observed. The excess of SOCl_2 was pumped off. The raw product was then purified by vacuum distillation. The fraction at 98 $^\circ\text{C}/10 \text{ mm Hg}$ was collected (14.14 g, 88% reaction yield). ^1H NMR (CDCl_3 , 200 MHz): δ 7.63 (d, 1H, $J = 5.1 \text{ Hz}$), 7.01 (d, 1H, $J = 5.1 \text{ Hz}$), 2.53 (s, 3H); ^{13}C NMR (CDCl_3 , 200 MHz): δ 16.8, 131.9, 132.9, 135.8, 150.1, 158.8; IR: ν/cm^{-1} 3102 (w), 2942 (w), 2924 (w), 1738 (s), 1512 (m), 1442 (w), 1390 (s), 1370 (s), 1256 (w), 1242 (w), 1198 (s), 1090 (w), 1030 (m), 950 (w), 854 (s), 800 (s), 742 (s), 666 (s), 630 (m), 596 (m).

***N,N'*-Bis(3-methylthien-2-ylcarbonyl)hydrazide (2).** Anhydrous pyridine (42 ml) and 2.2 ml of hydrazine monohydrate were consecutively added to a round bottom flask equipped with a dropping funnel and a back condenser. Then 13.6 g (0.0847 mol) of 3-methylthiophene-2-carbonyl chloride (**1**) were added dropwise to the reactor using the dropping funnel; the reaction mixture was boiled for 20 min, then cooled to room temperature, poured on ice, filtered and the filtered solid was washed with water. The raw reaction product was recrystallised from ethanol (8.02 g, 67.6% reaction yield). M.p. 175–176 $^\circ\text{C}$; ^1H NMR (CDCl_3 , 200 MHz): δ 7.36 (d, 2H, $J = 5.1$

Hz), 6.93 (d, 2H, $J = 5.1 \text{ Hz}$), 2.57 (s, 6H), 8.66 (s, 2H); ^{13}C NMR (CDCl_3 , 200 MHz): δ 15.8 (2C), 127.4 (2C), 128.2 (2C), 132.0 (2C), 143.1 (2C), 160.4 (2C); IR: ν/cm^{-1} 3222 (m, br), 3110 (w), 2996 (w), 2924 (w), 2846 (w), 1678 (m), 1640 (w), 1618 (s), 1510 (m), 1502 (s), 1482 (w), 1468 (w), 1442 (w), 1412 (s), 1380 (m), 1368 (m), 1326 (w), 1278 (s), 1230 (w), 1218 (s), 1104 (m), 1060 (w), 1032 (m), 944 (w), 912 (m), 892 (w), 878 (w), 852 (w), 824 (s), 744 (m), 714 (s), 688 (m), 638 (m), 606 (s), 566 (m); anal. calcd for $\text{C}_{12}\text{H}_{12}\text{N}_2\text{O}_2\text{S}_2$: C, 51.41%; H, 4.31%; N, 9.99%; S, 22.87%; found: C, 51.35%; H, 4.36%; N, 10.06%; S, 23.10%.

2,5-Bis(3-methylthien-2-yl)-1,3,4-oxadiazole (3). A mixture of 2.8 g (1 mmol) of *N,N'*-bis(3-methylthien-2-ylcarbonyl)hydrazide (**2**) and 8 ml of POCl_3 was boiled with constant stirring for 1 h. The excess of POCl_3 was then pumped off and the reaction mixture was poured on ice, filtered and the residue was washed with water. The raw product was purified by recrystallisation from ethanol (2.1 g, 81.0% reaction yield). M.p. 137–138 $^\circ\text{C}$; ^1H NMR (CDCl_3 , 200 MHz): δ 7.41 (d, 2H, $J = 5.0 \text{ Hz}$), 6.98 (d, 2H, $J = 5.0 \text{ Hz}$), 2.65 (s, 6H); ^{13}C NMR (CDCl_3 , 200 MHz): δ 16.0 (2C), 119.4 (2C), 128.6 (2C), 131.8 (2C), 142.1 (2C), 160.3 (2C); IR: ν/cm^{-1} 3100 (s), 2970 (w), 2940 (w), 2916 (m), 2848 (w), 2734 (w), 2616 (w), 1584 (m), 1564 (s), 1556 (m), 1538 (w), 1530 (m), 1514 (w), 1504 (m), 1494 (m), 1484 (w), 1470 (w), 1462 (w), 1444 (w), 1432 (w), 1426 (w), 1414; anal. calcd for $\text{C}_{12}\text{H}_{10}\text{N}_2\text{O}_2\text{S}_2$: C, 54.94%; H, 3.84%; N, 10.68%; S, 24.44%; found: C, 54.95%; H, 3.76%; N, 10.67%; S, 24.71%.

2,5-Bis(5-bromo-3-methylthien-2-yl)-1,3,4-oxadiazole (4). 2,5-Bis(3-methylthien-2-yl)-1,3,4-oxadiazole (**3**; 1.1 g, 4.9 mmol) was mixed with 1.56 g (8.77 mmol) of NBS in 10 ml CF_3COOH ; the solution was stirred for 18 h and then poured into water. The precipitate was filtered, dissolved in boiling ethanol and filtered again. The filtrate was then placed in a refrigerator for slow crystallisation of the reaction product. A second recrystallisation from ethanol yielded 0.68 g of the desired dibromo derivative (38.6% reaction yield). M.p. 129–130 $^\circ\text{C}$; ^1H NMR (CDCl_3 , 200 MHz): δ 6.97 (s, 2H), 2.60 (s, 6H); ^{13}C NMR (CDCl_3 , 200 MHz): δ 15.9 (2C), 116.6 (2C), 120.5 (2C), 134.4 (2C), 142.5 (2C), 159.2 (2C); IR: ν/cm^{-1} 3072 (w), 2920 (w), 2848 (w), 1564 (s), 1528 (m), 1518 (w), 1498 (s), 1462 (w), 1428 (m), 1410 (m), 1380 (w), 1354 (w), 1310 (w), 1250 (w), 1186 (w), 1092 (w), 1036 (m), 990 (w), 938 (w), 912 (m), 828 (m), 786 (w), 728 (m), 696 (w), 630 (w), 604 (w); anal. calcd for $\text{C}_{12}\text{H}_8\text{Br}_2\text{N}_2\text{O}_2\text{S}_2$: C, 34.31%; Br, 38.04%; H, 1.92%; N, 6.67%; S, 15.26%; found: C, 33.96%; Br, 38.17%; H, 1.92%; N, 6.55%; S, 14.96%.

2,5-Bis[5-(3-octylthien-2-yl)-3-methylthien-2-yl]-1,3,4-oxadiazole (5). 5,5-Dimethyl-2-(3-octylthien-2-yl)[1,3,2]dioxaborinane (760 mg, 2.46 mmol) and 2,5-bis(5-bromo-3-methylthien-2-yl)-1,3,4-oxadiazole (**4**; 470.5 mg, 1.12 mmol) were placed in anhydrous DMF (15 ml). The mixture was stirred under argon for 10 min and then 522 mg of K_3PO_4 (2.46 mmol) and 77.6 mg of $\text{Pd}(\text{PPh}_3)_4$ (0.672 mmol) in 15 ml of DMF were added. The mixture was kept for an additional period of 14 h at 90 $^\circ\text{C}$ with constant stirring and then allowed to cool to room temperature. After filtration, the solution was extracted with diethyl ether ($3 \times 25 \text{ ml}$) and the organic layer was washed with brine ($3 \times 25 \text{ ml}$). The combined organic layers were then dried over magnesium sulfate and filtered. The solvent was removed using a rotary evaporator and the crude product was purified by column chromatography over silica gel, eluting with mixtures of solvents of increasing polarity (pentane–methylene chloride 100:0 to 60:40). The blue luminescent waxy product was then recrystallised from chloroform and methanol at $-10 \text{ }^\circ\text{C}$ to give 50 mg of yellow crystals (10% reaction yield). ^1H NMR (CDCl_3 ,

200 MHz): δ 7.23 (d, 2H, $J = 5.24$ Hz), 7.00 (s, 2H), 6.96 (d, 2H, $J = 5.24$ Hz), 2.80 (t, 4H, $J = 7.66$ Hz), 2.66 (s and t, 6H), 1.60–1.75 (m, 4H), 1.25–1.45 (m, 20H), 0.83–0.90 (m, 6H); ^{13}C NMR (CDCl_3 , 200 MHz): δ 14.1 (2C), 16.1 (2C), 22.6 (2C), 29.2 (2C), 29.3 (2C), 29.4 (2C), 29.5 (2C), 30.6 (2C), 31.8 (2C), 118.5 (2C), 124.0 (2C), 129.4 (2C), 129.9 (2C), 130.3 (2C), 134.4 (2C), 139.5 (2C), 142.1 (2C), 160.3 (2C); IR: ν/cm^{-1} 3060 (w), 2942 (w), 2920 (s), 2850 (s), 1566 (s), 1536 (s), 1518 (w), 1496 (s), 1460 (w), 1452 (w), 1434 (w), 1406 (w), 1378 (m), 1258 (m), 1082 (m), 1036 (s), 926 (w), 918 (w), 870 (w), 830 (s), 798 (m), 728 (s), 688 (m), 652 (m), 630 (s), 608 (m); MS: $m/z = 651.1$ (M^+).

Electropolymerisation, electrochemical and spectroelectrochemical studies

Electropolymerisation experiments were performed in a one-compartment electrochemical cell using a platinum disc working electrode, a platinum counter electrode and an Ag/0.1 M AgNO_3 /acetonitrile reference electrode. The latter was calibrated *versus* ferrocene redox couple measured in the same electrolytic solution. The electrolytic solution used in the electropolymerisation consisted of 0.1 M tetrabutylammonium tetrafluoroborate (Bu_4NBF_4) in a 2:3 v/v mixture of methylene chloride and acetonitrile, to which an appropriate amount of the monomer was added to give a concentration of 1×10^{-2} M in the case of **3**, and 5×10^{-3} M in the case of **5**. The same electrochemical cell was used for cyclic voltammetry investigations of the polymer, the electrolyte consisting of 0.1 M Bu_4NBF_4 in acetonitrile. For spectroelectrochemical investigations, the polymer was deposited on an ITO transparent electrode using the same analytical conditions. The corresponding UV-vis-NIR spectra were obtained in a specially designed rectangular spectroelectrochemical cell and recorded in the increasing electrode potential mode, using a Lambda 2 Perkin Elmer spectrometer (wavelength range 280–1100 nm).

Results and discussion

Mixed heterocyclic oligomers containing an oxadiazole central ring have previously been prepared by Mitschke *et al.*⁷ in a search for new materials with tunable luminescent and electrochemical properties. These authors prepared end-capped thiophene-based pentamers with an oxadiazole central ring. The blocking of the C_α and the C_β positions in the terminal thiophene rings was intended to prevent electropolymerisation of the synthesised oligomers. To the contrary, the goal of our research was to obtain electropolymerisable thiophene-oxadiazole oligomers.

In the preparation of the mixed heterocyclic trimer **3**, we have applied a very similar synthetic pathway to that used in ref. 7 for the preparation of the end-capped pentamers. Thus, **3** is obtained from 3-methylthiophene-2-carboxylic acid in a three-step procedure that involves the formation of the corresponding carbonyl chloride **1**, followed by reaction with hydrazine to give the N,N' -diacylhydrazine derivative **2**. This inter-

mediate, upon dehydration, gives the mixed heterocyclic trimer with the oxadiazole central unit **3**.

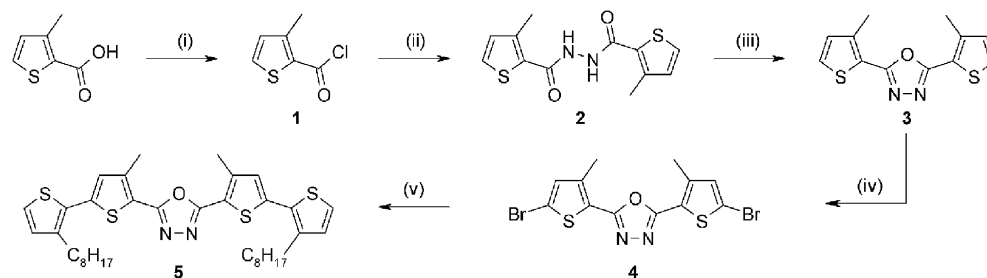
Synthesis of the pentamer **5** from the trimer requires two additional steps (Scheme 1). The first step consists in the bromination of **3**. The use of classical procedures [treatment with Br_2 or N -bromosuccinimide (NBS) in classical solvents] was unsuccessful. To achieve this reaction, the deactivated aromatic compound **3** was treated with NBS in trifluoroacetic acid solvent to give the corresponding dibromo aromatic compound **4** in reasonable yields. The applied procedure was quite similar to the procedure described in ref. 8. **5** is then obtained *via* Suzuki coupling, that is, the reaction of **4** with 5,5-dimethyl-2-(3-octylthien-2-yl)[1,3,2]dioxaborinane, the latter being prepared according to the literature⁹. Suzuki or Stille coupling are convenient methods not only for the preparation of alternating conjugated copolymers¹⁰ but also for the synthesis of regiochemically well-defined oligomers, which can then constitute building blocks for the preparation of polymers with tunable electronic, spectroscopic and electrochemical properties.¹¹

In Fig. 1 the UV-vis absorption spectra of the trimer **3** and the pentamer **5** are compared. As expected, the main band, ascribed to the $\pi\text{-}\pi^*$ transition in the conjugated π system, undergoes a significant bathochromic shift by *ca.* 55 nm when going from **3** to **5**. One must also note here that the $\pi\text{-}\pi^*$ transition band in the alkyl substituted mixed pentamer **5** is located at a shorter wavelength (371 nm) when compared to the same band (at 402 nm) for the end-capped unsubstituted analogue of **5** studied in ref. 7. This can be taken as a spectroscopic evidence of the chain torsion induced by the substituents.

Both **3** and **5** are photoluminescent (Fig. 2). The measured photoluminescence quantum yield for the trimer and the pentamer are 13% and 46%, respectively (see Table 1). In the latter case, it approaches that reported for the unsubstituted pentamer containing the oxadiazole central ring.⁷

Attempts to electropolymerise **3** were unsuccessful. Fig. 3 shows a voltammetric scan obtained in the Bu_4NBF_4 /acetonitrile electrolyte containing **3**. For this scan only, a strong, irreversible anodic peak can be observed with a maximum at $E = 1.37$ V, that is, in the potential range where the thiophene-based polyconjugated systems undergo oxidative degradation.¹² This degradation product passivates the electrode since, in the consecutive scan (not shown in Fig. 3), the intensity of the anodic peak decreases by *ca.* one order of magnitude. Such behaviour is a direct consequence of the electron-withdrawing character of the oxadiazole ring, which, *via* mesomeric and inductive effects, lowers the electron density in adjacent thiophene rings. As a consequence, the formation of a radical cation, which initiates the oxidative polymerisation of the trimer, is more difficult. The oxidation starts at very high potentials, leading to an unstable radical cation that undergoes several consecutive degradation reactions at the rate exceeding the desired polymerisation *via* $\text{C}_\alpha\text{-C}_\alpha$.

In the case of pentamer **5**, the effect of the electron-withdrawing properties of the central oxadiazole ring on the



Scheme 1 Synthetic pathway for the preparation of the mixed heterocyclic monomers **3** and **5**: (i) SOCl_2 , 2 h, reflux, 88% yield; (ii) pyridine, H_2NNH_2 , 20 min, reflux, 68% yield; (iii) POCl_3 , 1 h, reflux, 81% yield; (iv) NBS, CF_3COOH , 18 h, r.t., 39% yield; (v) 5,5-dimethyl-2-(3-octylthien-2-yl)[1,3,2]dioxaborinane, $\text{Pd}(\text{PPh}_3)_4$ (cat), K_3PO_4 , DMF, 14 h, 90 °C, 10% yield.

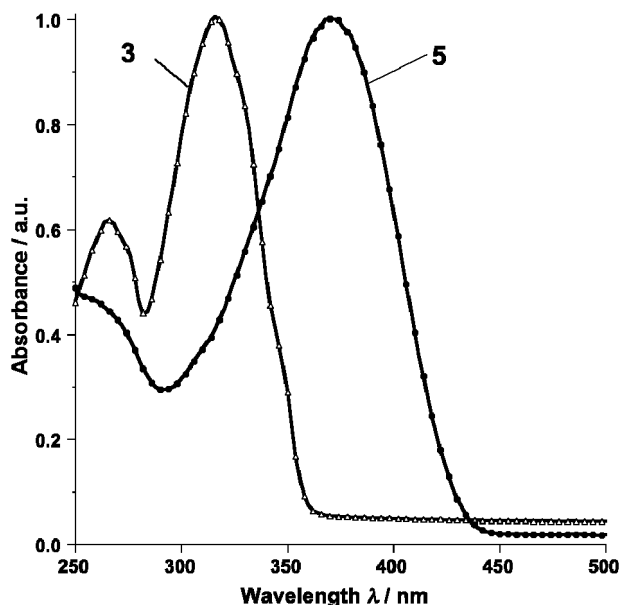


Fig. 1 UV-Vis absorption spectra of **3** (Δ) and **5** (\bullet) registered in chloroform solution.

reactivity of the terminal C_α carbons is much less pronounced and, as a result, the pentamer readily electropolymerises. Fig. 4 shows voltammetric behaviour of **5** dissolved in the Bu_4NBF_4 /acetonitrile electrolyte. Three independent scans were registered with increasing reverse potential: 1, 1.2 and 1.5 V, respectively. As clearly seen, the oxidation of **5** starts at $E < 0.9$ V with the formation of a polymer layer, which gives a clear cathodic peak on the reverse scan. This peak, attributed to the undoping of the polymer formed, is observed for scans limited to 1 and 1.2 V. The extension of the limiting potential to 1.5 V results in the oxidative destruction of the deposited polymer, which, in this case, shows no electrochemical activity in the reverse scan. Since the polymerisation anodic peak partially overlaps with the oxidative destruction peak, it is worthwhile to carry out the polymerisation at the lowest possible potential. Therefore, in further cyclic voltammetry polymerisations we have limited the reverse potential to $E = 0.9$ V. These conditions assure smooth deposition of the polymer on the electrode as seen in Fig. 5. The polymer growth is manifested by an increase in the intensity of the polymer doping/undoping redox

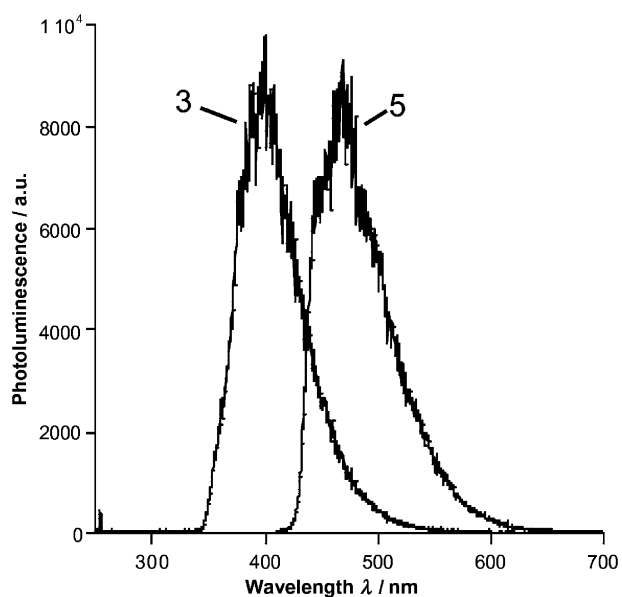


Fig. 2 Photoluminescence spectra of **3** and **5** registered in chloroform solution with excitation at 254 nm for **3** and at 400 nm for **5**.

Table 1 Optical properties of **3**, **5** and **P5**

Compound	$\lambda_{\max, \text{abs}}/\text{nm}^a$	$\lambda_{\max, \text{PL}}/\text{nm}^b$	Q_f^c
3	316	399	0.13 ± 0.03
5	371	467	0.46 ± 0.02
P5	431	528	0.33 ± 0.02
P5 (thin film)	545 (0 \rightarrow 0) 504 (0 \rightarrow 1) 472 (0 \rightarrow 2)	651	—

^a Absorption maxima in the UV-vis spectra from chloroform solution or thin film (as indicated). ^b Photoluminescence maxima from chloroform solution or thin film. ^c Quantum yield.

couple with each consecutive scan. In the subsequent text, the polymer obtained by voltammetric polymerisation of **5** will be denoted as **P5**.

After electropolymerisation, the deposited polymer layer was repeatedly rinsed with acetonitrile, with the goal to remove any pentamer **5** possibly adsorbed on the polymer surface, then reduced at the potential $E = 0.25$ V to give fully undoped (neutral) **P5**.

SEC investigations of neutral **P5** showed that the obtained product is a mixture of oligomers of **5** rather than a true polymer. The chromatogram shows a trimodal distribution with a dominant peak corresponding to 1337 Da, a second peak corresponding to 2450 Da and a third broad peak of very low intensity corresponding to higher molecular weights. Taking into account correction factors for the determination of molecular weights of polyconjugated systems by SEC with the use of polystyrene standards,¹³ we can conclude that **P5** is a mixture of dimers and higher oligomers of **5**.

In Fig. 6, the chloroform solution absorption and luminescence spectra of **P5** are shown. As expected, coupling *via* electropolymerisation induces a strong (60 nm) bathochromic shift in both the absorption and the photoluminescence bands (compare Figs. 2 and 6 and Table 1). The chloroform solution of **5** emits blue radiation whereas that of **P5** emits green radiation (33% quantum yield).

Solid state absorption and photoluminescence spectra of **P5** are shown in Fig. 7. The absorption spectrum shows a clear vibrational structure. The exact positions of the individual peaks originating from the fine structure, obtained through the second derivative analysis, are listed in Table 1. Vibrational structure in the solid state spectra of polyconjugated systems is

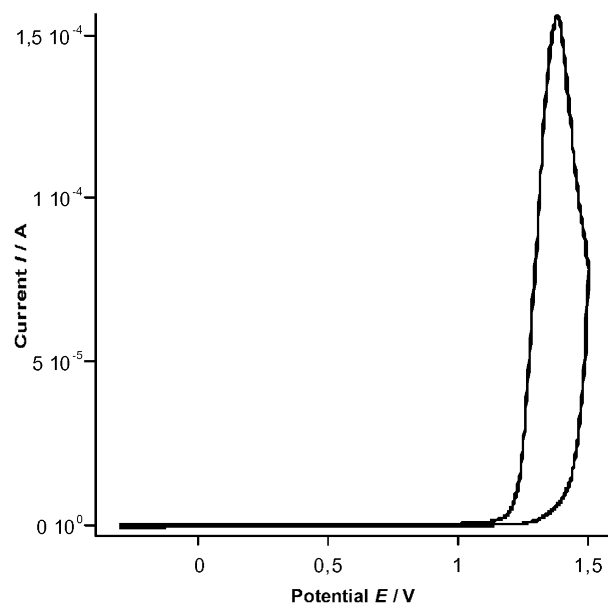


Fig. 3 Cyclic voltammogram of **3** in 0.1 M Bu_4NBF_4 in a 2:3 v/v mixture of methylene chloride and acetonitrile at 50 mV s^{-1} scan rate.

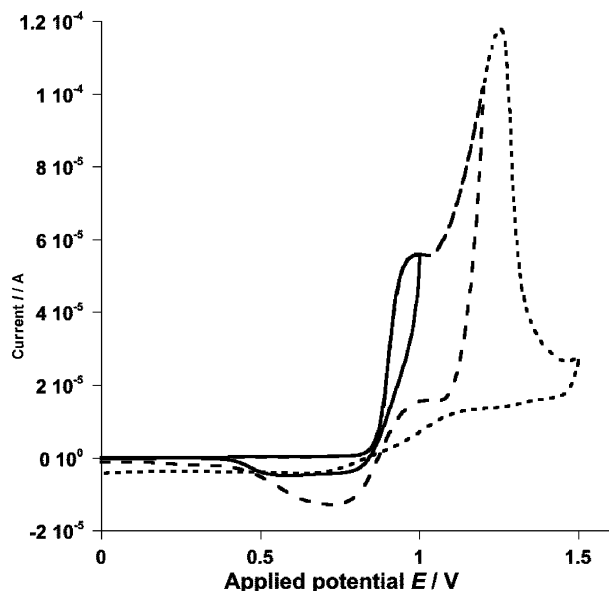


Fig. 4 Cyclic voltammety electropolymerisation of **5** in 0.1 M Bu₄NBF₄ in a 2:3 v/v mixture of methylene chloride and acetonitrile with different limiting potentials $E = 0.9$ V (solid line), 1.2 V (dashed line), and 1.5 V (dotted line); scan rate of 50 mV s⁻¹.

a typical manifestation of electron lattice coupling. The $0 \rightarrow 0$ transition, that is, the transition from the ground state to the relaxed excited state, is roughly inversely proportional to the conjugation length. It should be noted that in **P5** the band corresponding to this transition is significantly red-shifted as compared to the corresponding band in the solid state spectrum of the acetone fraction of regioregular poly(3-hexylthiophene), which shows a comparable molecular weight and, consequently, comparable chain length.¹⁴ This means that neither the insertion of the oxadiazole ring nor the presence of the alkyl substituents in the head-to-tail, tail-to-tail coupling sequence (HT-TT, see inset in Fig. 5) perturb, to a significant extent, the conjugation in **P5**. The energy difference between the first and the second shoulders of the vibrational peak structure is 1540 cm⁻¹, which corresponds well to the Raman

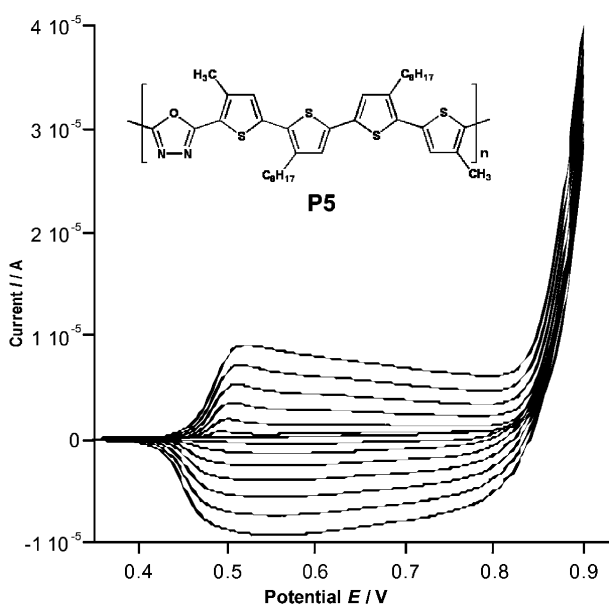


Fig. 5 Cyclic voltammety electropolymerisation of **5** to give **P5** at the limiting potential $E = 0.9$ V in 0.1 M Bu₄NBF₄ in a 2:3 v/v mixture of methylene chloride and acetonitrile; scan rate of 50 mV s⁻¹. Inset: chemical structure of polymer **P5**.

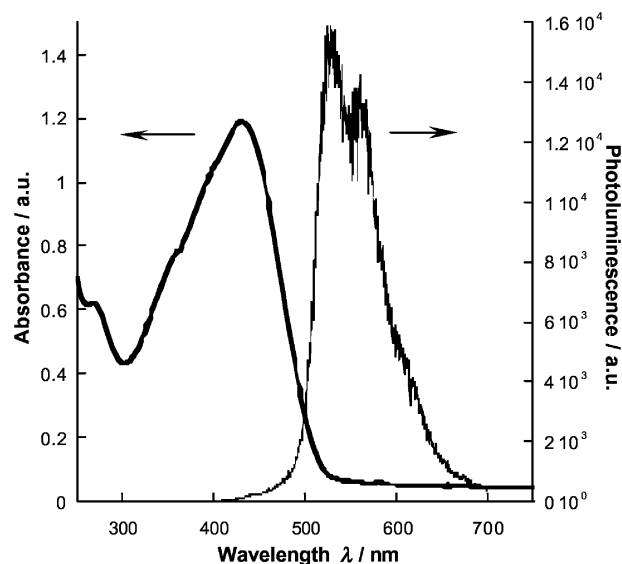


Fig. 6 UV-Vis absorption and photoluminescence spectra of **P5** recorded in chloroform solution with an excitation wavelength of 400 nm.

active mode of C=C antisymmetric stretching in the alkyl-substituted 2,5-thienylene ring.

In both its absorption and emission spectra, **P5** is solvatochromic. Its solid state photoluminescence band is red-shifted by 123 nm with respect to the corresponding band recorded for the chloroform solution (see Table 1). This large shift can be considered as indicative of π -stacking phenomena in the solid state, which, in turn, may negatively influence the solid state photoluminescence quantum yield. In any case, all data concerning the solid state spectra presented here must be considered as preliminary since they are not quantitative.

Fig. 8 shows cyclic voltammograms of **P5** recorded at different scan rates in Bu₄NBF₄/acetonitrile electrolyte. The oxidative doping/reductive undoping redox couple is clearly visible with anodic and cathodic peak maxima at 0.62 and 0.56 V, respectively, at a scan rate of 20 mV s⁻¹. The positions of both peaks are only slightly dependent on scan rate. The capacitive current plateau at potentials exceeding the anodic peak is indicative of efficient p-type doping and high polymer conductivity in the doped state.¹⁵

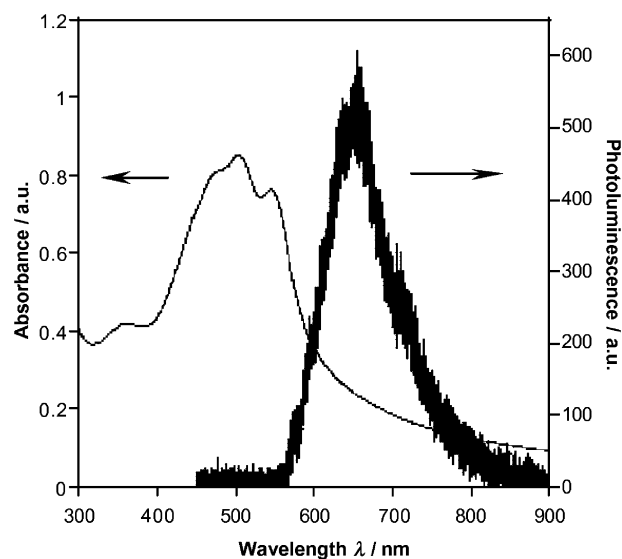


Fig. 7 UV-Vis absorption and photoluminescence spectra of a thin film of **P5** deposited on ITO at the excitation wavelength of 365 nm.

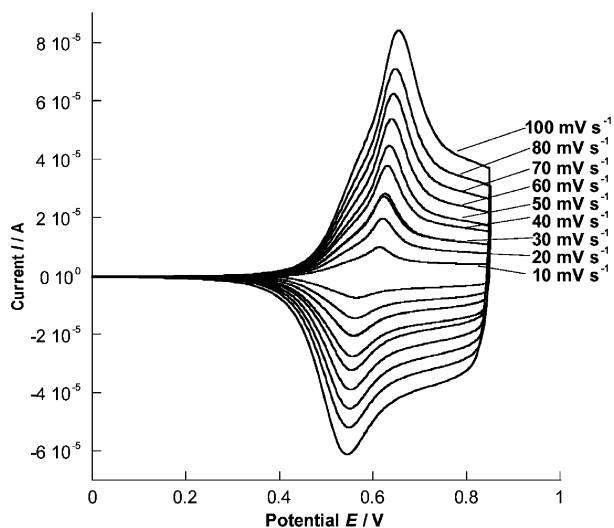


Fig. 8 Cyclic voltammograms of **P5** in 0.1 M Bu_4NBF_4 /acetonitrile at different scan rates between 10 and 100 mV s^{-1} .

The effect of the presence of the oxadiazole unit in the chain of **P5** is manifested here by a significantly higher potential of the anodic peak corresponding to the oxidative doping, as compared to poly(alkylthiophene) homopolymers of similar chain length and the same sequence of substituent distribution. Evidently, the electron-withdrawing properties of oxadiazole make the oxidation of the adjacent 2,5-thienylene units first to radical cations (polarons) and then to dications (bipolarons), more difficult.

Electrochemical oxidative doping of conjugated polymers results in a gradual bleaching of the band ascribed to the π - π^* transition with simultaneous growth of two new bands at higher wavelengths, associated with the formation of bipolarons (dications). For this reason, it is convenient to follow the electrochemical doping by spectroelectrochemistry. Doping-induced spectral changes of a thin layer of **P5**, deposited on an ITO electrode, are presented in Fig. 9.

Since the spectral range of the spectrometer used is limited to 1100 nm, only the higher energy bipolaron band and the onset of the lower energy one are seen. Spectral changes induced by the oxidative doping start to appear at $E = 0.55$ V, which is consistent with the cyclic voltammetry investigations, which show a small but nonzero current at this potential. At $E = 0.875$ V, the band originating from the π - π^* transition is

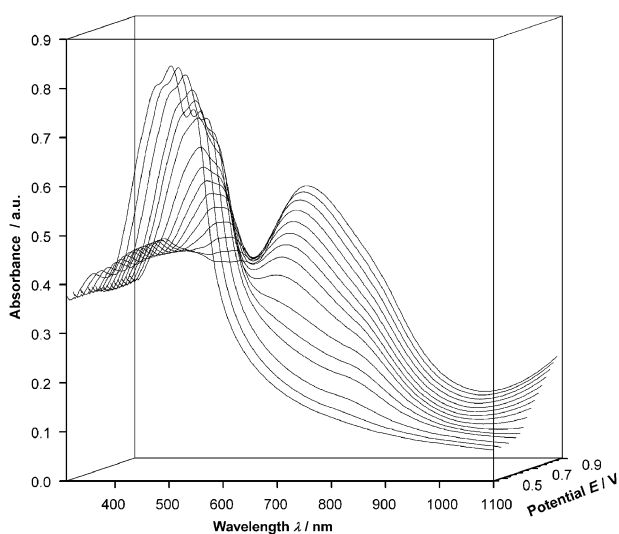


Fig. 9 UV-Vis-NIR spectra of **P5** recorded at increasing electrode potential E versus Ag/Ag^+ with 0.1 M Bu_4NBF_4 /acetonitrile electrolytic solution.

completely bleached, indicating the maximum doping level, which is confirmed by a high value of the capacitive current observed at this potential in the cyclic voltammogram of **P5** (compare Figs. 8 and 9). The bipolaron band, ascribed to the transition from the valence band to the second bipolaron level, appears at relatively short wavelengths ($\lambda_{\text{max}} = 644$ nm). This could be interpreted as a consequence of the rather low molecular weight of **P5**. For conjugated polymers of low molecular weight, the band gap is dependent on the chain length, increasing as the length decreases. As a consequence, the band associated with the transition from the valence band to the second bipolaron level appears at higher energies for short chain polymers. This was demonstrated in the case of fractionated regioregular poly(3-alkylthiophene),¹⁴ for which the higher energy bipolaron band continuously shifted towards higher wavelengths with increasing M_n , in the molecular weight range 2000–5400 Da. For higher M_n values, its position stabilised.

Conclusion

To summarise, we have prepared a mixed heterocyclic pentamer consisting of a central oxadiazole unit and of four alkylthiophene rings. The pentamer shows strong photoluminescence and electrochemical activity. Electrochemical oxidative coupling of the pentamer leads to a short chain polymer emitting red light. Its electrochemical and spectroelectrochemical properties are modified as compared to poly(alkylthiophene) homopolymers of comparable molecular weight, as a consequence of the electron-withdrawing properties of the oxadiazole unit.

Acknowledgements

The authors thank Dr Patrice Rannou for performing the SEC measurements. One of the authors (A.F.) wants to acknowledge the financial support of Joseph Fourier University in Grenoble in the form of a visiting professor fellowship.

References

- See for example: (a) *Handbook of Conducting polymers*, eds. T. A. Skotheim, R. L. Elsenbaumer and J. R. Reynolds, Marcel Dekker, 1998; (b) *Handbook of Organic Conductive Molecules and Polymers*, ed. H. S. Nalva, John Wiley, 1997.
- (a) Z. Bao, *Adv. Mater.*, 2000, **12**, 227–230; (b) A. C. Kraft, A. C. Grimsdale and A. B. Holmes, *Angew. Chem., Int. Ed.*, 1998, **37**, 402–428; (c) G. Yu, J. C. Hummelen, F. Wudl and A. J. Heeger, *Science*, 1995, **270**, 1789–1791.
- (a) B. Adhikari and S. Majumdar, *Prog. Polym. Sci.*, 2004, **29**, 699–766; (b) M. Schäferling and P. Bäuerle, *J. Mater. Chem.*, 2004, **14**, 1132–1141.
- (a) K. Kaeriyama, M. Sato and S. Tanaka, *Synth. Met.*, 1987, **18**, 233–236; (b) S. Hotta, *Synth. Met.*, 1987, **22**, 103–113; (c) M. Bouachrine, J. P. Lère-Porte, J. J. E. Moreau and M. Wong Chi Man, *J. Mater. Chem.*, 1995, **5**, 797–799; (d) Y. Zhu and M. O. Wolf, *Chem. Mater.*, 1999, **10**, 2995–3001; (e) A. Naji, M. Cretin, M. Persin and J. Sarrazin, *J. Appl. Polym. Sci.*, 2004, **91**, 3947–3958.
- (a) N. H. S. Lee, Z. K. Chen, S. J. Chua, Y. H. Lai and W. Huang, *Thin Solid Films*, 2000, **363**, 106–109; (b) S. Y. Song, T. Ahn, H. K. Shim, I. S. Song and W. H. Kim, *Polymer*, 2001, **42**, 4803–4811.
- (a) W. Huang, H. Meng, W. L. Yu, J. Gao and A. Heeger, *Adv. Mater.*, 1998, **10**, 593–596; (b) H. Meng and W. Huang, *J. Org. Chem.*, 2000, **65**, 3894–3901; (c) W. Huang, W. L. Yu, H. Meng, J. Pei and S. F. Y. Li, *Chem. Mater.*, 1998, **10**, 3340–3345; (d) Y. Chen, Y. Y. Huang and T. Z. Wu, *J. Polym. Sci., Part A: Polym. Chem.*, 2002, **40**, 2927–2936.
- (a) U. Mitschke, T. Debaerdemaeker and P. Bäuerle, *Eur. J. Org. Chem.*, 2000, 425–437; (b) U. Mitschke, E. Mena Osteritz, T. Debaerdemaeker, M. Sokolowski and P. Bäuerle, *Chem.-Eur. J.*, 1998, **4**, 2211–2224.
- D. J. Duan, L. H. Zhang and W. R. Dolbier, *Synlett.*, 1999, **8**, 1245–1246.

- 9 G. Bidan, A. De Nicola, V. Enée and S. Guillerez, *Chem. Mater.*, 1998, **10**, 1052–1058.
- 10 (a) M. Bouachrine, J. P. Lère-Porte, J. J. E. Moreau, F. Serein Spirau, R. A. Da Silva, K. Lmimouni, L. Ouchani and C. Dufour, *Synth. Met.*, 2002, **126**, 241–244; (b) J. P. Lère-Porte, J. J. E. Moreau, F. Serein Spirau, C. Torrelles, A. Righi, J. L. Sauvajol and M. Brunet, *J. Mater. Chem.*, 2000, **10**, 927–932; (c) F. Embert, J. P. Lère-Porte, J. J. E. Moreau, F. Serein Spirau, A. Righi and J. L. Sauvajol, *J. Mater. Chem.*, 2001, **11**, 718–722; (d) M. Jayakannan, J. L. J. van Dongen and R. A. J. Janssen, *Macromolecules*, 2001, **34**, 5386–5393; (e) U. Asawapirom, R. Güntner, M. Forster, T. Farrell and U. Scherf, *Synthesis*, 2002, **9**, 1136–1142; (f) J. Huang, Y. Niu, W. Yang, Y. Mo, M. Yuan and Y. Cao, *Macromolecules*, 2002, **35**, 6080–6082; (g) B. Liu, W. L. Yu, Y. H. Lai and W. Huang, *Macromolecules*, 2000, **33**, 8945–8952.
- 11 (a) W. L. Huang and Y. H. Lai, *Thin Solid Films*, 2002, **417**, 211–214; (b) M. Jayakannan, P. A. van Hal and R. A. J. Janssen, *J. Polym. Sci., Part A: Polym. Chem.*, 2002, **40**, 251–261; (c) J. P. Sauvage, J. M. Kern, G. Bidan, B. Divisia-Blohorn and P. L. Vidal, *New J. Chem.*, 2002, **26**, 1287–1290.
- 12 B. Krische and M. Zagorska, *Synth. Met.*, 1989, **28**, 263–268.
- 13 R. Demadrille, P. Rannou, J. Bleuse, J.-L. Oddou, A. Pron and M. Zagorska, *Macromolecules*, 2003, **36**, 7045–7054.
- 14 M. Trznadel, A. Pron, M. Zagorska, R. Chrzaszcz and J. Pieli-chowski, *Macromolecules*, 1998, **31**, 5051–5058.
- 15 J. Tanguy, A. Proń, M. Zagorska and I. Kulszewicz-Bajer, *Synth. Met.*, 1991, **45**, 81–105.